PAN
POLSKA AKADEMIA NAUK

JOURNAL OF WATER AND LAND DEVELOPMENT
e-ISSN 2083-4535

Study the local scour around different shapes of single submerged groyne

Budoor M. RASHAK ⬤ ✉, Saleh I. KHASSAF ⬤

University of Basrah, College of Engineering, Department of Civil Engineering, Centre of Basrah, Iraq

Abstract

River training structures; such as submerged groynes are low profile linear structures that are generally located on the outside bank to form groynes fields and prevent the erosion of stream banks by keeping a flow away from it. In the present research, the maximum scour depth was measured based on laboratory experiments where different shapes of submerged groynes (I-shape, L-shape, T-shape) were used as sort of countermeasures to investigate about most shapes that reduce the scour around them. The result of submerged groynes showed a clear decrease in scour depth ratio due to increasing submerged ratio and increase the scour hole geometry with increasing of flow intensity, and also Froude number. The maximum scour hole in this research was observed at T-shape groyne and then followed by I-shape groyne and L-shape groyne. The maximum scour depth that cased by I-shape was more than L-shape by a percentage about 8.2%, and it was less than T-shape by a percentage about 16.4%.

Key words: *bed materials, bed topography pattern, local scour, single submerged groyne*

INTRODUCTION

The problem of scour around any obstruction put in the alluvial channel is of great importance to hydraulic engineers. Practically, a channel is frequently obstructed by a means or other, for example, abutment. Groynes, spur-dikes, bridge piers, etc.

The percent study is concerned with local scour and deposition around submerged groynes, submerged groyne are flow diversion structures, commonly installed it's in a river where river depth is very deep. Their submergence condition different according to the water surface level in the river.

In many rivers, flooding happens various times a year causing most groynes to become submerged. The height of the submerged groyne crest is usually chosen carefully so that it does not construct too high can lead to an unnecessary high flow resistance at flood conditions, while a crest construct too low reduces the ability of the groynes to confine the flow at normal water levels. Therefore, the height of submerged groyne crest can be considered of as a design parameter optimized to investigate the main purpose of these obstructions. They include directing flow away from the river banks, and control river meandering and flooding. They may serve an additional function, such as improving aquatic habitats by creating low-velocity pools around their toes where fish can rest and nourish, improving channel navigation depth by contracting a wide shallow river, also increase the sediment transport rate (e.g., organic matter and suspended particulates) all through the submerged groyne reach, which reduces channel dredging costs [KASHYAP *et al.* 2014]. The local scour around submerged groynes is a common phenomenon in river engineering, it considers a difficult problem that has great significance to hydraulic researchers and also should be studied extensively. The hydrodynamics of the flow around a submerged groyne is far more complicated as part of the flow advected at the groyne area divides into an overflow that is advected over the groyne crest.

Therefore, the complexity of the problem warrants more works; both analytical and experimental during the design of such structures. The present research can be utilized to understand the structure of the horseshoe vortex system around the maximum upstream groyne at the initiation of the scour process. To form a vortex system in front of the obstruction which is swept downstream by the channel flow. Viewed from the top, this vortex system has the characteristic geometry shape of a horseshoe. therefore, is known a horseshoe vortex. Wake vortices form at the downstream side of the submerged groyne and are the consequence of flow separation at the sides of the groyne (Fig. 1).
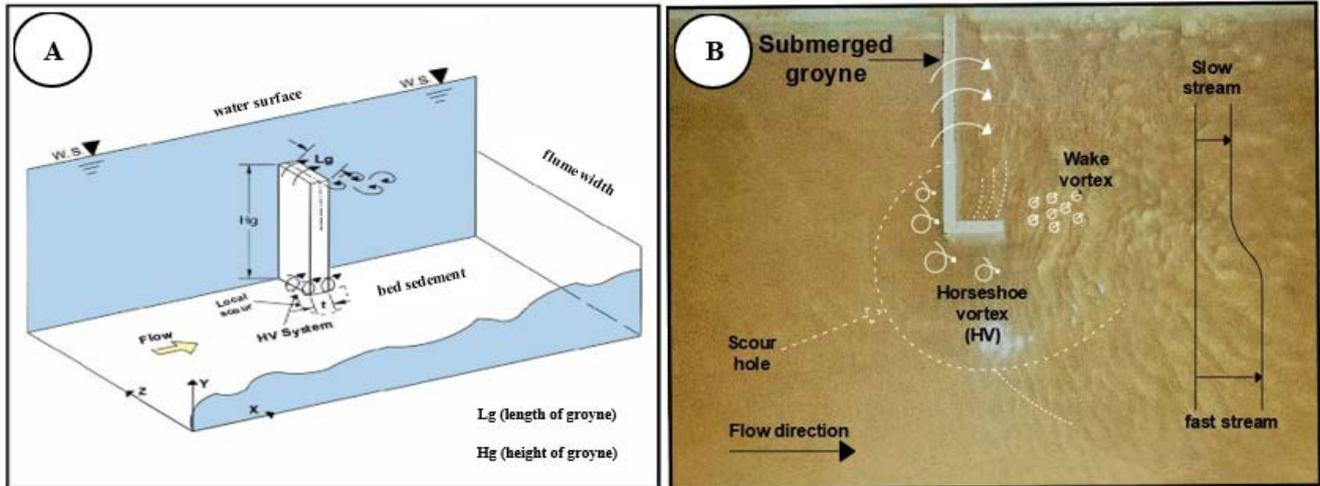
Fig. 1. The system of horseshoe vortex (HV): A) around single submerged groyne, B) during the run; source: own elaboration

These are called cast-off vortices and have vertical axes. One vortex develops on one side, sheds away and is transported to the downstream. Promptly, other forms on the other side, lastly shedding also. The wake vortices dissipate during they move down the flow [GHOSH 2018]. Overall, the effect of groyne submergence made the flow more complex, if the submergence is relatively deep, the overtopping flow remains comparatively parallel to the flow direction in the flume near the free surface while around the groynes field strong re-circulatory motions are present. The flow velocity over the roof interface is mostly higher than the mean flume velocity and crests as the overflow are adverted over the crests of the groynes, so the re-circulatory motions practically absent near the free surface at high submergence levels while it presents in the emerged case near the free surface [MCCOY et al. 2007].

In some of the test cases thought as (relatively low submergence depth) it was shown that the momentum that enters the groyne domain through the vertical mixing layer can obstruct the recirculating pattern. Subsequently, the flow inside the groyne field becomes relatively parallel to the flow in the flume and then a while shifts back to a recirculating pattern until another strong overtopping event to take place [MCCOY 2006].

Local scour parameters which influence the magnitude of scour depth at groyne: including flow intensity, flow depth, the shape of obstruction, shear and mean velocity depends on the equilibrium between flow bed erosion and sediment deposition, based on the mode of sediment transport [LAGASSE, RICHARDSON 2001].

Two different scour regimes have been determined, clear-water scour and live-bed scour. The flow velocity (v) measured in the laboratory experiment should be less than the critical velocity (v_c) of bedload.

The scour develops first and subsequently, continue until the scour hole dimensions no longer increase and the depth of scouring reaches a specific value that is the maximum scour depth. And the live bed scour happens for the general transition of the material of bed by the flow and the approach flow velocity (v) becomes more than the beginning of motion (v_c) [HONG et al. 2012]. Then the scour hole is reached strong highly but it disperses with time since the sediments enter from upstream, consequ ently; leaves the scour hole [KIRAGA, POPEK 2016].

MATERIAL AND METHODS

MATERIALS

The experimental flume. The flume utilized in this study, as shown in Figures 2 and 3. It is made of fibreglass reinforced plastic with steel reinforcement, with 5.64 m length, 0.6 m width and having a depth of 0.4 m.
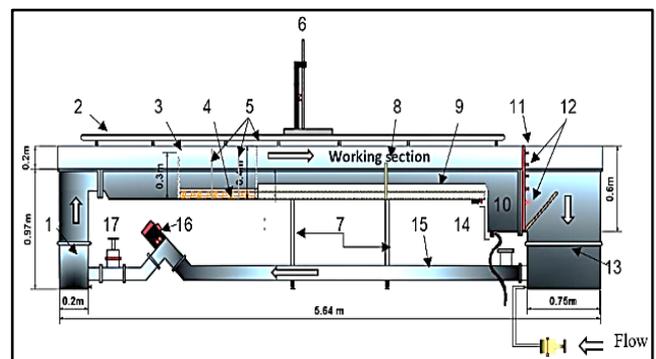

Fig. 2. The laboratory flume; source: own elaboration

Fig. 3. Detail drawing of a laboratory flume; 1 = inlet tank, 2 = rail, 3 = weir, 4 = gravel, 5 = screens, 6 = point gate, 7 = two support, 8 = model, 9 = sand bed, 10 = sediment basin, 11 = tailgate, 12 = walves to control the tailgate, 13 = reservoir tank, 14 = drain, 15 = pipe 10-cm diameter, 16 = centrifugal pump, 17 = regulating wave; source: own elaboration

The flume made of three sections: the first section consists of an inlet tank situated in the upstream of the flume with measurements of 0.2×1.17×0.6 m for length, depth and width respectively. The second section of the flume is the working section consists of the sharp-crested rectangular weir 0.6 m width and 0.35 m height used to measure flow discharge, gravel and screens to distributed the flow uniformly over the whole width of the flume and helped in dissipating the excess energy of flow and prevent the entering of debris and any undesirable particles into the flume working section. In the middle layer of sand of 0.1 m thickness and 2.35 m length, at the end of working section a sediment basin 0.4×0.3 m for length and depth respectively, the flow depth is controlled by a tailgate supplier with ten wheels' levels. The third section of the flume is a reservoir 0.75×1.17×0.6 m for the length, depth and width respectively, which provided the water through a recirculating flume of the closed water system by a centrifugal pump. The centrifugal pump attached with an electric motor of maximum capacity equals 8.4 dm^3·s^{-1}.

The experimental models. Submerged groyne models were utilized in all the experiments, the models were made of polystyrene foam material of thickness 1 cm and height H_g 15 cm of which 5 cm is the net height (height of submerged groyne should have between 1/3 and 1/2 of water depth) [JHA, KARMACHARYA 2000]. And 20 cm projection length Lg (approximately not less than one-third of the flume width) [MÖWS, KOLL 2019] with different shapes of groynes (I-shape, L-shape, T-shape) as appeared in Figures 4 and 5.
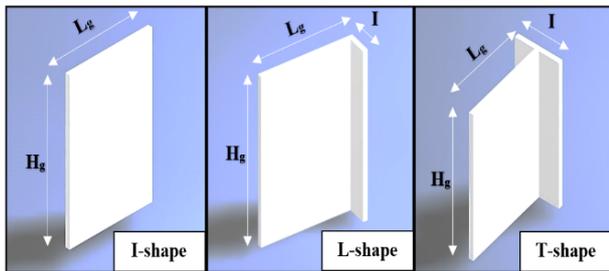

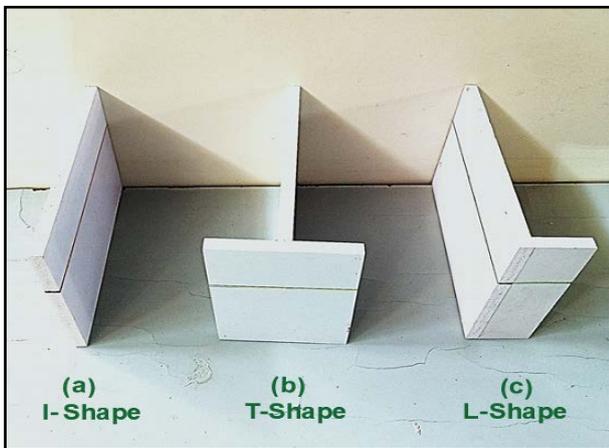Fig. 4. Sketches for the groynes models' shapes: source: own elaboration

Fig. 5. Different shapes of groynes model; source: own elaboration

The models were fixed vertically in the sand layer where they put in the middle of the working section of the flume to achieve a well-established flow. A silicon adhesive was utilized to fixed immediately the groynes to the inner sidewall of the flume. Figure 6 displays a groyne placed in the flume before starting the tests.
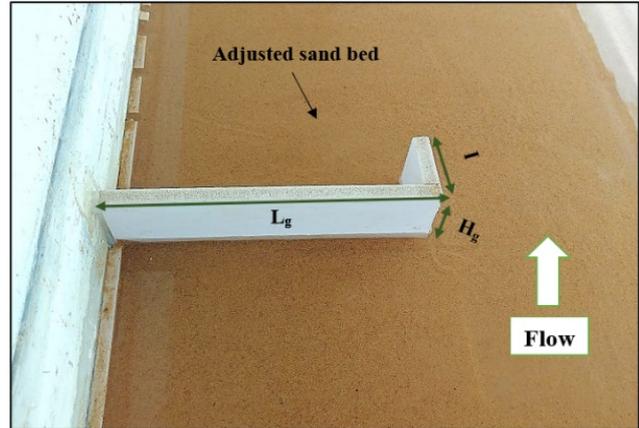

Fig. 6. Groyne placed in the flume; own elaboration

The bed materials. In this study, a mechanical sieve analysis was conducted to classification the sand bed material as a bed flume. Sieving analysis was carried out at the laboratory of soil in Civil Engineering Department, Basrah University to obtain the characteristics of the sand bed. In the tests showed that the bed material consists of cohesionless sand with the mean partial size of $d_{50} = 0.3$ mm, d_{50} is taken as a delegate particle size of sediment, and the level of uniformity distribution particle size is characterized by the geometric standard deviation of $\sigma_g = 1.32$; σ_g is expressed as $\sigma_g = \sqrt{d_{84} : d_{16}}$. It is usually accepted that the sediment may be considered uniform if $\sigma_g < 1.4$ and no uniform else [ZHANG, NAKAGAWA 2008]. The value of the standard deviation infers that the utilized sand is of uniform size and the results include the effect of sediment of non-uniformity to eliminate the decrease of the local scour that expected to occur due to armouring impact in non-uniform sand. Figure 7 explains the grain size distribution curve.
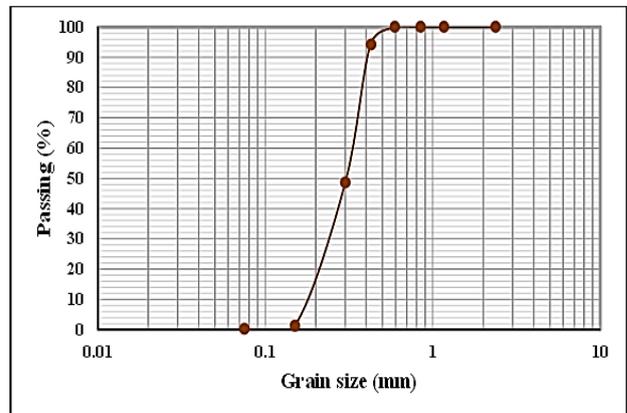

Fig. 7. Distribution curve of grain size for bed material $d_{50} = 0.3$ mm; source: own study

METHODS

Time of the equilibrium. The time needed to find the equilibrium conditions of scour to be used in all tests is important to know it for avoiding the impact of the time and introduced an equilibrium time at 95% of the end scour [MELVILLE, CHIEW 1999]. Several experimental runs were carried out. Five various velocities were utilized and the scour was recorded at a specified time interval spans by using a point gauge to measure the maximum scour depth at the nose of the upstream groyne. From Figure 8 the depth of scouring is sharply increased in the first third of the test period, then the development of scour depth with the time has become almost constant. It should be aforementioned that v is expressed as the average velocity of flow while vc is express as the average velocity at the primary motion of the bed sediment of flow. Besides, it has been noticed that about 95% of the local scour depth accomplished in 2-hours. For more accuracy, the time is lasted as 3-hours for all test runs.
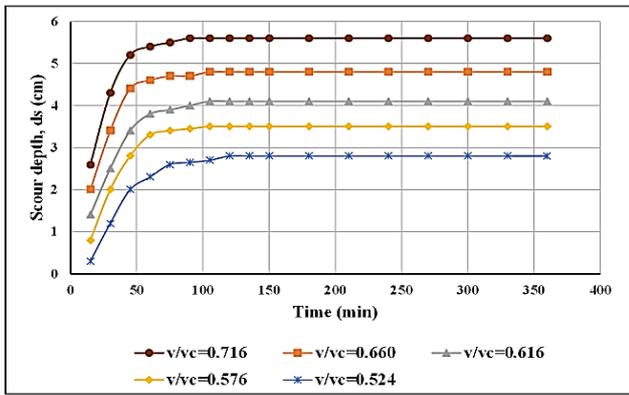

Fig. 8. Development of scour depth with the time using L-shape groyne; source: own study

Dimensionless parameters on local scour around submerged groyne. The parameters that are affected on the local scour around the submerged groyne and experimental runs depend on there are following as below, currently; using dimensional analysis; the maximum scour depth ($d_{S\max}$) can be written in the utilitarian functional as follows:

$$d_{S\max} = f\{h_0, h_1, H_g, v, v_c, L_g, \rho, \rho_s, g, d_{50}, \mu, \sigma_g, B, S_0, I, \theta\} \quad (1)$$

$$\therefore f_1\{d_{S\max}, h_0, h_1, H_g, v, v_c, L_g, \rho, \rho_s, g, d_{50}, \mu, \sigma_g, B, S_0, I, \theta\} = 0 \ (2)$$

All the factors definitions are listed in Table 1.

Table 1. The factors definitions using in dimensional analysis

Symbol	Definition	Dimension
B	flume width	L
I	projection length of groyne parallel to the flow direction	L
L_g	projection length of groyne	L
H_g	height of groyne	L
d_{16}	sediment size for which 16% of the particle are finer	L
d_{50}	median particle grain size	L
d_{84}	sediment size for which 84% of the particle are finer	L

d_S	local scour depth around the groyne	L
Fr	Froude number	–
g	gravitational acceleration	$L \cdot t^{-2}$
S_0	the slope of channel bed	–
h_0	flow water depth	L
h_1	distance from the water surface to the top of the groyne	L
θ	the angle of groyne inclination	–
v	mean velocity	$L \cdot t^{-1}$
v_c	critical velocity	$L \cdot t^{-1}$
σ_g	geometric standard deviation	–
μ	dynamic viscosity of the fluid	$M \cdot t^{-1} \cdot L^{-1}$
ρ	density of fluid	$M \cdot t^{-3}$
ρ_s	the density of the sediment	$M \cdot t^{-3}$

Source: own elaboration.

The dimensional analysis method that used in this research is the Buckingham's π theorem where the number of the fundamental units (m) that must be provided are mass (*M*), length (*L*), and time (*t*). Since there are seventeen factors (*n* = 17) involving three essential units (*m* = 3), the quantity of dimension-less parameter should be (*n* – *m*) = (17 – 3) = 14 terms, thus;

$$f_2\{\pi_1, \pi_2, \pi_3, \pi_4, \pi_5, \pi_6, \pi_7, \pi_8, \pi_9, \pi_{10}, \pi_{11}, \pi_{12}, \pi_{13}, \pi_{14}\} = 0 \ (3)$$

In each term; the variables number is (*m* + 1); that is (3 + 1) = 4. By taking (ρ, v, h_0) as the repeating variables; and the same way for all keeps the parameter taking each term:

$$\pi_1 = \rho^{a1} v^{b1} h_0^{c1} d_{S\max}$$
$$\pi_2 = \rho^{a2} v^{b2} h_0^{c2} v_c$$
$$\pi_3 = \rho^{a3} v^{b3} h_0^{c3} L_g$$

And the same way for all keeps the parameter taking each term,

$$\pi_1 = \rho^{a1} v^{b1} h_0^{c1} d_{S\max}$$

By expression these in dimension terms by using *M*, *L* and *T* system:

$$M^0 \cdot L^0 \cdot T^0 = (M \cdot L^{-3})^{a1} \cdot (L \cdot T^{-1})^{b1} \cdot (L)^{c1} \cdot L$$

$M: 0 = a_1$	$a_1 = 0$
$L: 0 = -3a_1 + b_1 + c_1$	$b_1 + c_1 = 0$
$T: 0 = -b_1$	$b_1 = 0$ and $c_1 = -1$

$$\pi_1 = \rho^0 v^0 h_0^{-1} d_{S\max} \Longrightarrow \quad \pi_1 = \frac{d_{S\max}}{h_0}$$

By the same procedure:

$$\pi_2 = \frac{h_1}{h_0} \qquad \pi_3 = \frac{H_g}{h_0} \qquad \pi_4 = \frac{v}{v_c}$$
$$\pi_5 = \frac{L_g}{h_0} \qquad \pi_6 = \frac{\rho_s}{\rho} \qquad \pi_7 = Fr$$
$$\pi_8 = \frac{d_{50}}{h_0} \qquad \pi_9 = \frac{\mu}{\rho v h_0} \qquad \pi_{10} = \sigma_g$$
$$\pi_{11} = \frac{B}{h_0} \qquad \pi_{12} = S_o \qquad \pi_{13} = \frac{I}{h_0}$$
$$\pi_{14} = \theta$$

$$\therefore 0 = f_3\left(\frac{d_{S\max}}{h_0}, \frac{h_1}{h_0}, \frac{H_g}{h_0}, \frac{v}{v_c}, \frac{L_g}{h_0}, \frac{\rho_s}{\rho}, Fr, \frac{d_{50}}{h_0}, \frac{\mu}{\rho v h_0}, \sigma_g, \frac{B}{h_0}, S_o, \frac{I}{h_0}, \theta\right)$$

Then, the simplification of the above relationship by dispensing with the terms with constant values and applying the assumption: (1) constant sediment size, (2) constant groyne dimensions (length and height of projection length of groyne parallel to the flow direction), (3) relative density, (4) steady viscosity, (5) horizontal channel floor with-

out any inclination and constant channel width. Therefore, the factional relationship may be written as:

$$f_4\{\pi_1, \pi_2, \pi_4, \pi_7\} = 0 \text{ or}$$

$$f_4 \left\{ \frac{d_{Smax}}{h_0}, \frac{h_1}{h_0}, \frac{v}{v_c}, \text{Fr} \right\} = 0 \qquad (4)$$

The maximum depth of scour:

$$\frac{d_{Smax}}{h_0} = f_5 \left\{ \frac{h_1}{h_0}, \frac{v}{v_c}, \text{Fr} \right\} \qquad (5)$$

By the same the functional relationships which describe scouring depth normalized with flow depth for all groyne shapes may be written as:

$$\frac{d_{Smax}}{h_0} = f_6 \left\{ \frac{h_1}{h_0}, \frac{v}{v_c}, \text{Fr} \right\} \qquad (6)$$

This equation and its parameters will be used in laboratory experiments.

RESULTS AND DISCUSSION

Discussing and analysing the results acquired from the laboratory data is a most important step in designing the submerged groynes, to reduce the scour depth created around them, the experiments are categorized according to their purposes in Table 2. And all the experimental work was performed in steady subcritical flow and clear water conditions to inspect the scour phenomenon, the geometrical measurements for all experimented models used in the study are listed in Table 3.

Table 2. Summary of experiments

Runs	Description
1–5	tested the flow intensity of and Froud number utilizing single I-shape groyne
6–10	tested the submerged ratio using single I-shape groyne
11–15	tested the flow intensity of and Froud number using single L-shape groyne
16–20	tested the submerged ratio using single L-shape groyne
21–25	tested the flow intensity of and Froud number using single T-shape groyne
26–30	tested the submerged ratio using single T-shape groyne

Source: own study.

Effect of flow intensity (v:v_c) on the local scour (d_S:h_0). It is an important parameter that effect on the scour around submerged groynes. Five different velocities were utilized in the experiments and observed that the scour depth increased linearly with flow velocity increasing at values for all parameters remaining constant.

It can be noticed from Figures 9 and 10 that the flow intensity will increase the scour hole width and volume and the location of the hole will shift so it will surround the groyne from both sides, this may be attributed to the increase in separation zone that situated in the downstream side of the submerged groyne. More vortexes will be created that in turn causing more scour.

Effect of Froude number (Fr) on the local scour (d_S:h_0). The results of the I-shape, L-shape, T-shape submerged groynes have been shown in Figure 11.
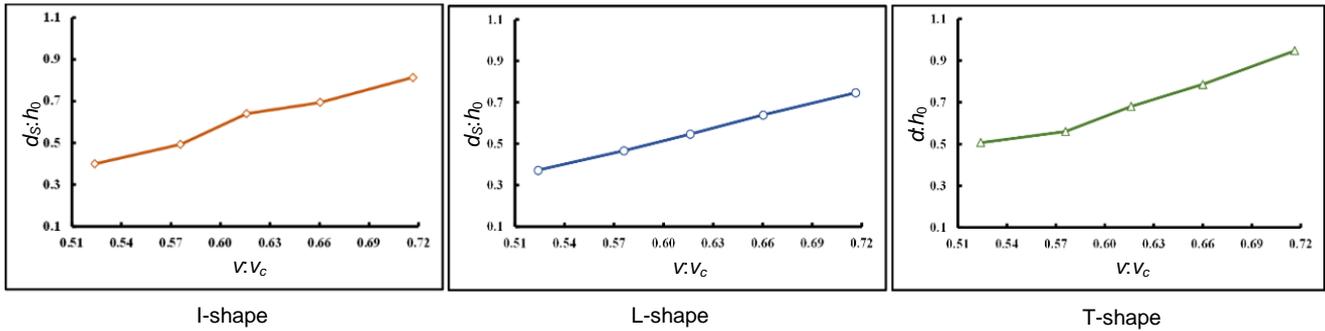
Table 3. The experimental results

Run No.	Model name	h_0 (cm)	h_1 (cm)	v (m·s⁻¹)	v_c (m·s⁻¹)	Fr	h_1:h_0	v:v_c	d_S (cm)	d_S:h_0
1		7.5	2.5	0.179	0.250	0.208	0.33	0.716	6.1	0.81
2		7.5	2.5	0.165	0.250	0.192	0.33	0.660	5.2	0.69
3		7.5	2.5	0.154	0.250	0.180	0.33	0.616	4.8	0.64
4		7.5	2.5	0.144	0.250	0.168	0.33	0.576	3.7	0.49
5	I-shape	7.5	2.5	0.131	0.250	0.153	0.33	0.524	3.0	0.40
6		11	6	0.179	0.263	0.172	0.55	0.680	3.4	0.31
7		10	5	0.179	0.259	0.180	0.50	0.691	4.3	0.43
8		9	4	0.179	0.256	0.190	0.44	0.699	5.2	0.58
9		8	3	0.179	0.252	0.202	0.38	0.710	5.8	0.73
10		7	2	0.179	0.247	0.216	0.29	0.724	6.3	0.90
11		7.5	2.5	0.179	0.250	0.208	0.33	0.716	5.6	0.75
12		7.5	2.5	0.165	0.250	0.192	0.33	0.660	4.8	0.64
13		7.5	2.5	0.154	0.250	0.180	0.33	0.616	4.1	0.55
14		7.5	2.5	0.144	0.250	0.168	0.33	0.576	3.5	0.47
15	L-shape	7.5	2.5	0.131	0.250	0.153	0.33	0.524	2.8	0.37
16		11	6	0.179	0.263	0.172	0.55	0.680	2.3	0.21
17		10	5	0.179	0.259	0.180	0.50	0.691	3.0	0.30
18		9	4	0.179	0.256	0.190	0.44	0.699	4.3	0.48
19		8	3	0.179	0.252	0.202	0.38	0.710	5.0	0.63
20		7	2	0.179	0.247	0.216	0.29	0.724	6.2	0.89
21		7.5	2.5	0.179	0.250	0.208	0.33	0.716	7.1	0.95
22		7.5	2.5	0.165	0.250	0.192	0.33	0.660	5.9	0.79
23		7.5	2.5	0.154	0.250	0.180	0.33	0.616	5.1	0.68
24		7.5	2.5	0.144	0.250	0.168	0.33	0.576	4.2	0.56
25	T-shape	7.5	2.5	0.131	0.250	0.153	0.33	0.524	3.8	0.51
26		11	6	0.179	0.263	0.172	0.55	0.680	3.9	0.35
27		10	5	0.179	0.259	0.180	0.50	0.691	5.0	0.50
28		9	4	0.179	0.256	0.190	0.44	0.699	5.7	0.63
29		8	3	0.179	0.252	0.202	0.38	0.710	6.5	0.81
30		7	2	0.179	0.247	0.216	0.29	0.724	7.4	1.06

Explanations: parameters' symbols as in Tab. 1.
Source: own study.

Fig. 9. Effect of flow intensity (v:v_c) on development of scour depth ratio (ds:h_0) for different shapes of submerged groynes; v = mean velocity, v_c = critical velocity, ds = local scour depth around the groynes, h_0 = flow water depth; source: own study
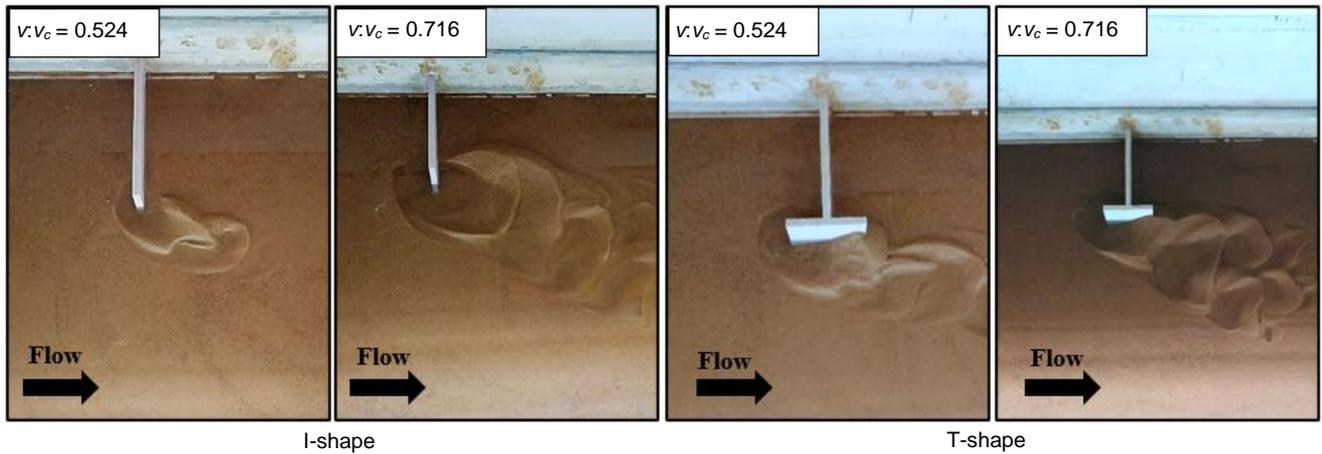

Fig. 10. The effect of flow intensity (v:v_c) on scour depth development (ds:h_0); v, v_c, ds, h_0 as in Fig. 10; source: own study
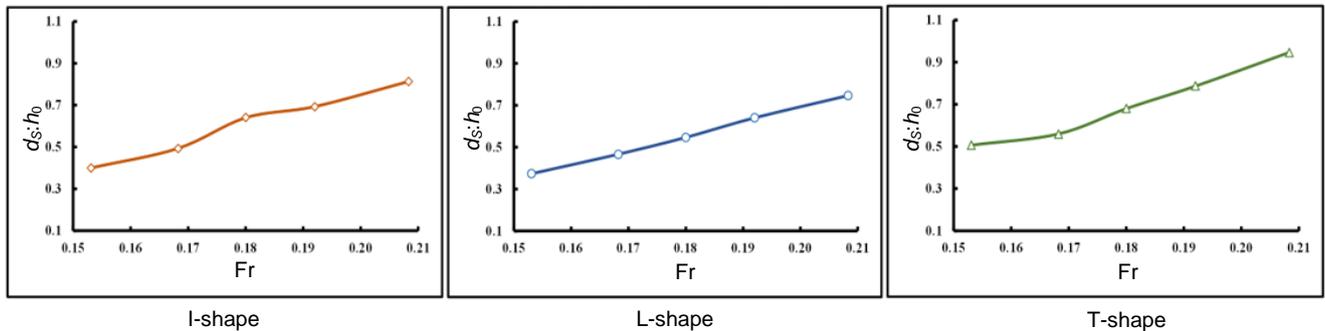

Fig. 11. Effect of Froude number (Fr) on development of scour depth ratio (ds:h_0) for different shapes of submerged groynes; d_S, h_0 as in Fig. 10; source: own study

dimensionless fraction (d_S:h_0) any increase in Froude number will increase the depth of scour at surely constant for all parameters value.

Figure 12 presents the impact of increasing Froude number from 0.153 to 0.208. It can be seen that scour process occur in the wider and larger region, besides; when Fr = 0.153 the fewer sediments were distributed around the scour hole with small camber.

While, when Fr = 0.208 the sediments will collect around the scour hole sides with very high camber, then the sediments starts to reduce and gradually disappear at the far downstream of the submerged groyne.

Effect of submerged ratio (h_1:h_0) on the local scour (d_S:h_0). The effect of submerged ratio on the scour is very important around submerged groynes. Five different experiments were carried out under the same flow conditions

and observed that the scour depth decrease linearly with flow submerged ratio increasing at values with all parameters remaining constant. As shown in Figure 13, it is shown that the overtopping flow does make a significant difference in the magnitude of scour depth, in which increasing the submerged ratio is inversely proportional to the scour depth ratio. This result is illustrated obviously in Figure 14. It is evident that due to the re-circulatory motions practically absent near the free surface at high submergence levels, and it will decrease the ability of horseshoe vortices to pick up and entrain sediments. So; when there flows that can be described as deep; the holes of local scour are decreased until they become having invisible efficiency, while it presents in low submergence level case strongly near the free surface causing an increase of scour hole.
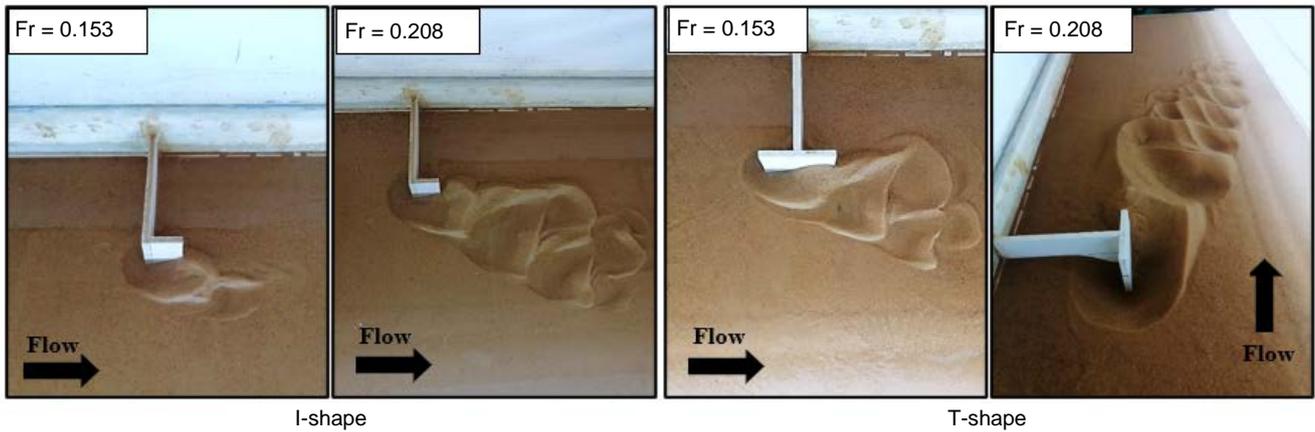
Fig. 12. The effect of Froude number (Fr) on the ratio of scour depth development (d_S:h_0); d_S, h_0 as in Fig. 10; source: own study
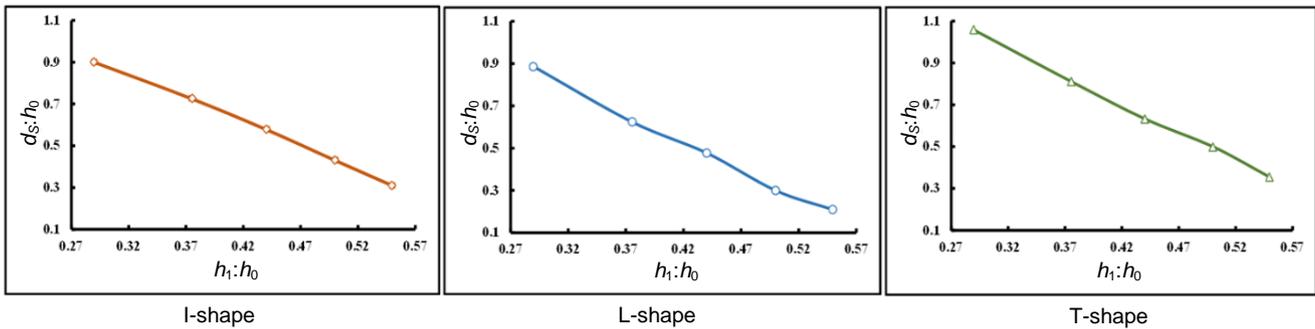

Fig. 13. Effect of submerged ratio (h_1:h_0) on development of scour depth ratio (d_S:h_0) for different shapes of submerged groynes; h_1, h_0, d_S, h_0 as in Fig. 10; source: own study
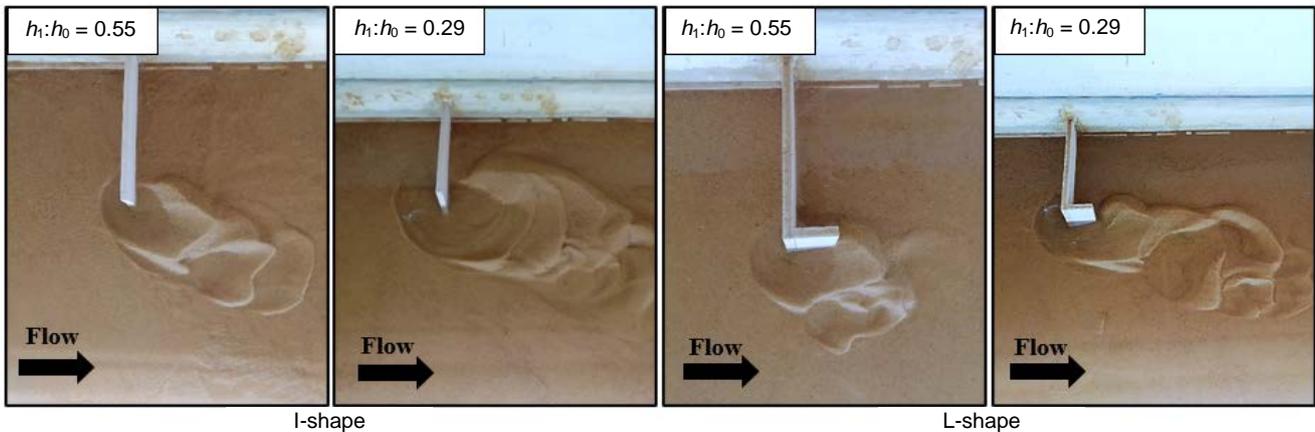
Fig. 14. Photos that clarify the effect of submerged ratio (h_1:h_0) on the ratio of scour depth development (d_S:h_0); d_S, h_1, h_0, as in Fig. 10; source: own study

Comparison of local scour between the shapes of the groynes. It has been investigated the influence of three shapes of submerged groynes (I-shape, L-shape, and T-shape) on the scour depth process. Under the same hydraulic conditions and for the same effecting parameters, for restricting only the impact of changing the shape on the scour development. Figure 15 relates with the maximum scour depth development with various groyne shape for the different parameters. it is observed from these figures the scour depth ratio for the (T-shape) type will be as maximum value as compared with the least value when the groyne shape is (L-shape) type. The L-shape had the potential to decrease the velocity in the wake region of the structure more effectively than the I-shape and T-shape. that is due to the L-shape extension absorbs the energy near the downstream of the groyne and distributes it over a wider region, while blockage of sediment movements occurs behind the groyne by decreasing in the intensity of eddies resulting in strengthening of the bank against the erosive. Single submerged groynes can be arranged from the shape that gives maximum scour hole values to that give minimum scour hole values as T-shape, I-shape, L-shape where the maximum scour depth that cased by I-shape was more than L-shape by a percentage about 8.2%, and it was less than T-shape by a percentage about 16.4%, under the same conditions of maximum Froude number.
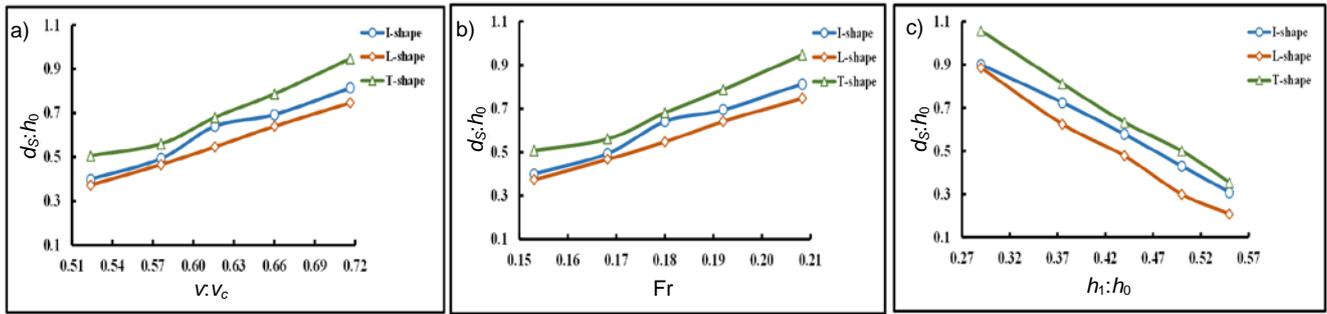
Fig. 15. The effect of scour depth ratio (d_S:h_0) with different groynes shapes for the different parameters: a) flow intensity (v:v_c), b) Froude number (Fr), c) submerged ratio (h_1:h_0); d_S, h_0, h_1, v, v_c, as in Fig. 10; source: own study
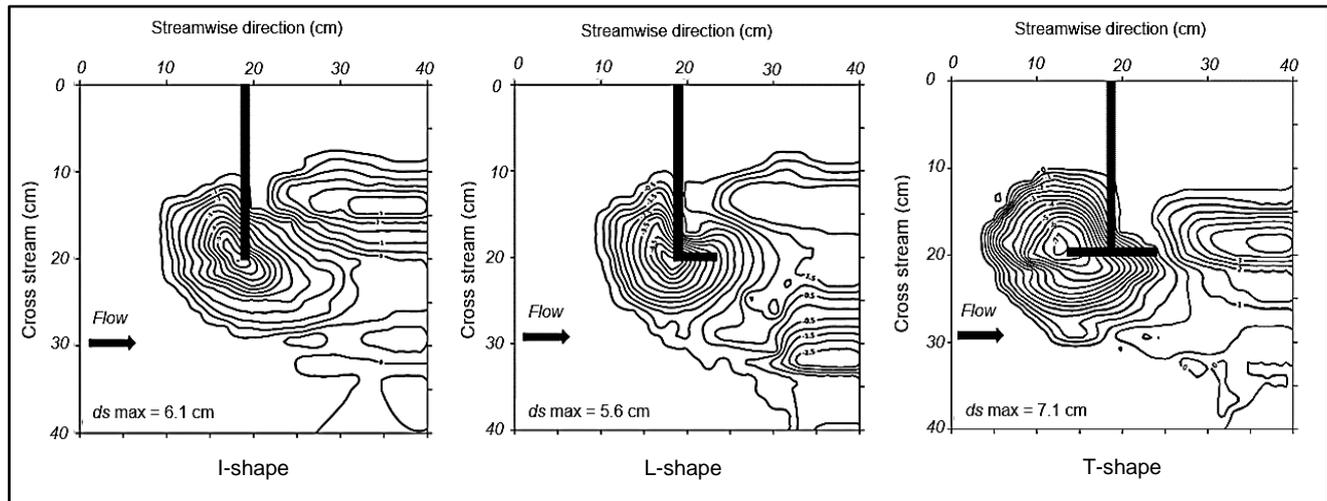

Fig. 16. Contour maps for scour holes submerged groynes in different shape for the cases of maximum discharge; d_S as in Fig. 10; source: own study

Bed topography pattern. After the end for chosen experiments of maximum discharge, to the comparison between scour patterns for submerged groyne, the data for bed sand topography level indicator are processed for drawing a contour map by utilizing the computer software (surfer 17). Figure 16 shows three shapes of graphs illustrating the topography of scour holes and downstream sand bars, each shape has similar flow conditions, submerged groyne geometry, and soil properties. The graphs for submerged groyne show that the maximum depth of scour at the upstream nose of the T-head shape. The shape of the scour hole upstream of the groyne was conical. while downstream, it was elongated and had a shallower slope. And the range width of scour depth in front of the groyne was 1–2 cm. The height of the sand ripples behind the groyne was observed to be about 2.5–3.5 cm, also scour and volume for L-shape submerged groyne is smaller than that for those I-shape, and T-shape groyne, while each shape using in this study formed sand bars in the downstream, however, bed sand waves for experiments of T-shape groynes extended longer distance in the downstream

CONCLUSIONS

This study is focused on characterizing the diversity in the behaviour of the flow and bed topography near sub-merged groynes. The flowing conclusions are outlined in the study that the maximum geometry of the scour hole is begun from the upstream side of the submerged groyne and stretch out to reach some distance in the downstream side; i.e.; where the maximum scours depth was observed to be at the upstream nose of submerged groyne because of its interception to the flow. The effect of various parameters on controlling scour around the submerged groyne was investigated. The results obtained showed that maximum scour depth was observed with increasing of flow intensity, Froude number. While increasing of submerged ratio could decrease the dimensions of scour depth. From the contour maps may be observed, scour hole width and volume for L-shape submerged groyne is smaller than that for those I-shape, and T-shape groyne, while each shapes using in this study formed sand bars in the downstream, however, bed sand waves for experiments of T-shape groynes extended longer distance in the downstream. The shape of the scour hole upstream of the groyne was conical. while downstream, it was elongated and had a shallower slope. Single submerged groyne can be arranged from the shape that gives maximum scour hole values to that give minimum scour hole values as T-shape, I-shape, L-shape where the maximum scour depth that cased by I-shape was more than L-shape by a percentage about 8.2%, and it was less than T-shape by a percentage about 16.4% under the same conditions of maximum Froude number.

REFERENCES

GHOSH T. 2018. Scour analysis around a flow centered vane dyke of different shape. MSc. Thesis in water resources and hydraulic engineering. West Bengal. India. Jadavpur University. No. M4WRE18008. pp. 72.

HONG Y.M., CHANG M.L., LIN H.C., KAN Y.C., LIN C.C. 2012. Experimental study on clear water scour around bridge piers. In: Applied Mechanics and Materials. Vol. 121 p. 162–166. DOI 10.4028/www.scientific.net/AMM.121-126.162.

JHA H., JHA S., KARMACHARYA B. 2000. Flood control measures best practices report. An approach for community-based flood control measures in the Terai rivers. Kathmandu. German Technical Cooperation.

KIRAGA M., POPEK Z. 2016. Using a modified Lane's relation in local bed scouring studies in the laboratory channel. Acta Scientiarum Polonorum Formatio Circumiectus. Vol. 5 (4) p. 209–226. DOI 10.15576/ASP.FC/2016.15.4.209.

KASHYAP S., RENNIE C.D., TOWNSEND R., CONSTANTINESCU G., TOKYAY T.E. 2014. Flow around submerged groynes in a sharp bend using a 3D LES mode. In: River flow 2010. Eds. A. Dittrich, K. Koll, J. Aberle, P. Geisenhainer. ISBN 978-3-939230-00-7 p. 643–650.

LAGASSE P.F., RICHARDSON E.V. 2001. ASCE compendium of stream stability and bridge scour papers. Journal of Hydraulic Engineering. ASCE. Vol. 127. Iss. 7 p. 531–533.

MCCOY A.W. 2006. Numerical investigations using LES: Exploring flow physics and mass exchange processes near groyne. PhD Thesis. University of Iowa. Vol. 48. No. 461 pp. 275. DOI 10.17077/etd.vt63cy20.

MCCOY A., CONSTANTINESCU G., WEBER L. 2007. A numerical investigation of coherent structures and mass exchange processes in channel flow with two laterals submerged groynes. Water Resources Research. Vol. 43. No. 5 p. 1–26. DOI 10.1029/2006WR005267.

MELVILLE B.W., CHIEW Y.M. 1999. Time scale for local scour at bridge piers. Journal of Hydraulic Engineering. Vol. 125. Iss. 1 p. 59–65. DOI 10.1061/(ASCE)0733-9429(1999)125:1(59).

MÖWS R., KOLL K. 2019. Roughness effect of submerged groyne fields with varying length, groyne distance, and groyne types. Water. Vol. 11. No. 6. p. 1–11. DOI 10.3390/w11061253.

ZHANG H., NAKAGAWA H. 2008. Scour around spur dyke. Journal of Advanced and Future Researches. Japan. No. 51b p. 633–652.